Direct simulation of turbulent combustion

By T. J. Poinsot

Problem background and objectives

Understanding and modeling of turbulent combustion are key-problems in the computation of numerous practical systems. Because of the lack of analytical theories in this field and of the difficulty of performing precise experiments, direct simulation appears to be one of the most attractive tools to use in addressing this problem.

The present work can be split into two parts:

1. Development and validation of a direct simulation method for turbulent combustion.

2. Applications of the method to premixed turbulent combustion problems.

The goal of part 1 is to define and to test a numerical method for direct simulation of reacting flows. A high level of confidence should be attached to direct simulation results, and this can only be achieved through extensive validation tests. We have considered two major questions :

1.1. Which equations should be solved? Contrary to cold-flow turbulence, the choice of equations to solve for turbulent reacting systems is still an open question. At the present time, it is not reasonable to compute time-dependant solutions of Navier-Stokes equations with complex chemistry in multi-dimensional configurations. A reduction in the number of equations to be solved is needed. This also leads to a loss of information which must be estimated.

1.2. Which configurations should be studied and what boundary conditions are necessary? A second problem is the choice of the configurations to study and of the associated boundary conditions. Most direct simulations of cold-flow turbulence are performed for temporal situations with periodic boundary conditions. This approach is not convenient for many reacting flows, and spatial simulations are required. These simulations can not be done without adequate boundary conditions.

In part 2, direct simulation is used to address some of the many critical problems related to turbulent combustion. At the present time, I have limited this work to premixed combustion and considered only four basic issues :

2.1. The effect of pressure waves on flame propagation.

2.2. The interaction between flame fronts and vortices. This is the basic problem of turbulent combustion. The goal here is to gain more insight into the fundamental interaction mechanisms between flame fronts and vortices.

2.3. The influence of curvature on premixed flame fronts.

2.4. The validation of flamelet models for premixed turbulent combustion.

Questions 2.1 to 2.3 concern fundamental processes in turbulent premixed combustion which are not well understood at the present time. Part 2.4 is related to modeling and its goal is to use results obtained in sections 2.2 and 2.3 to construct and validate a flamelet model for turbulent premixed flames.

1. Development and validation of a direct simulation method for reacting flows

1.1. The equations to solve

The amount of complexity to include in direct simulations of reacting flows requires difficult compromises. Taking into account the variations of thermodynamical properties with temperature and chemical compositions as well as solving for all species present in a reacting compressible flow will typically lead to codes slower by at least three orders of magnitude than the codes used presently for cold flows. This is due to the high number of additional equations to solve (around 30 for a propane flame) but also to the stiffness of the resulting equations which will need very dense computation grids. On the other hand, using constant density assumptions, infinitely fast chemistry approximation or oversimplified equations for species concentrations (like assuming that the Lewis number is equal to unity, in which case the species concentration may be obtained directly from the temperature) will lead to faster codes but will not tell us much about real mechanisms. The choice which was made here is the following (Poinsot and Lele 1989):

- solve the complete Navier-Stokes equations, including variable density and compressibility effects,
- use an elementary reaction for premixed combustion (*Reactants* $\rightarrow$ *Products*) and finite rate chemistry (Arrhenius law). The reaction rate $\dot{w}_R$ is expressed as:

$$\dot{w}_R = B\rho Y_R \ \exp\left(-\frac{T_{ac}}{T}\right) \tag{1}$$

where T_{ac} is the activation temperature and Y_R is the local mass fraction of reactants.

- solve separately for species concentration and temperature (non-unity Lewis number),
- take into account the variations of species diffusion, viscosity and conductivity with temperature,
- take into account heat losses.

This choice is accompanied by certain limitations:

- the Schmidt, Prandtl and Lewis numbers are fixed,
- most cases are run in two-dimensional geometries,
- only premixed combustion has been considered.

Extensions to three-dimensional or to diffusion flames are straightforward. At the present stage, the following mechanisms can be described:

- dynamic effect of the flame front on the flow (this requires variable density),
- effects of the flow on the inner structure of the flame front (this requires finite-rate chemistry),
- extinction of the flame by stretch and influence of curvature (this requires non-unity Lewis numbers and non-zero heat losses),
- influence of pressure waves on combustion, triggering of combustion instabilities (this requires compressibility).
- mixing, ignition, and quenching mechanisms in supersonic combustion (this requires compressibility, non-unity Lewis number, and finite-rate chemistry).
- flame-generated vorticity and flame/vortex interactions (this requires non-constant density and viscosity).

All these mechanisms are key-processes in many combustion phenomena and few of them are well understood in a general sense. Before going to three-dimensional cases with more complex chemistry, the present approach can lead to many original and important results.

1.2. Configurations and boundary conditions

A second problem is the choice of the configurations to study and of the associated boundary conditions. An extensive study of appropriate boundary conditions for spatial direct simulation has been performed. This effort goes beyond the scope of reacting flows, and its goal is to provide a satisfactory method to specify boundary conditions in cases where periodicity can not be assumed. Periodicity has been used in most direct simulations of reacting or non-reacting flows because it suppresses the need of boundary conditions (The domain is folded on itself). When more realistic problems are considered (involving inflows and outflows, for example) the problem of boundary conditions becomes crucial. On the basis of methods proposed for the Euler equations (Thompson 1987), a general formulation for the Navier Stokes equations has been derived (Poinsot and Lele 1989). This method called Navier-Stokes Characteristic Boundary Conditions (NSCBC) applies for most boundaries (inlet, outlet, adiabatic slip-wall, no-slip adiabatic, or isothermal wall). It has been implemented in the high-order finite-difference code of Dr. Lele and tested in the following configurations (all of them concern spatially evolving flows) :

1/ Non-reacting shear layers (confined by walls or unconfined).
2/ Premixed flames in a shear layer.
3/ Acoustic waves leaving the computation domain (subsonic and supersonic).
4/ Vortices leaving the computation domain (subsonic and supersonic).
5/ Very low Reynolds number flows (Poiseuille flow).

As an example, Figs. 1 and 2 show results obtained from test 4. A vortex is generated at time $t = 0$ in a supersonic flow and is convected downstream. The mean flow is uniform, from left to right at a Mach number of $u_0/c = 1.1$ (c is the sound speed). The maximum velocity induced by the vortex is small ($0.0018u_0$). The plots on the left side of Figs. 1 and 2 give the vorticity field

while the plots on the right side display the longitudinal velocity perturbations $(u - u_0)/u_0$. The right boundary is supposed to be 'non-reflecting'. It should let the vortex pass through without generating any perturbation. Two methods were used for the outlet boundary:

- Method 1 is a reference method proposed by Rudy and Strikwerda (1981) which can be viewed as the prototype of methods used by many other authors (Yee 1981, Jameson and Baker 1984). It uses extrapolation for the velocities and the density. The pressure is then obtained by solving for a Riemann invariant and relaxing the pressure to some value at infinity.
- Method 2 is the 'non-reflecting' version of the NSCBC method.

Supersonic outlet boundary conditions are supposed to be easy to implement because no information can travel upstream towards the inlet. All errors created at the outlet should be convected outwards. In fact, physical information satisfies this assumption but numerical instabilities do not (Vichnevetsky and Pariser 1986). Using extrapolation at the outlet generates numerical waves which travel upstream much faster than the sound speed and interact with the inlet to generate other perturbations (Poinsot, Colonius and Lele 1989). This coupling is very strong with method 1 (Fig. 1). Not only is the vorticity field near the outlet strongly modified but the inlet field is also affected and additional vorticity is introduced into the computation. The total vorticity and the maximum vorticity in the domain do not go to zero after the vortex has left the domain (Fig. 3). This numerical feedback between outlet and inlet can lead to non-physical instabilities similar to the one described by Buell and Huerre for incompressible flows (1988) and could make the final results of the simulation dubious.

When the NSCBC method is used, the vortex leaves the domain without any perturbation. The total vorticity and the maximum vorticity in the computation box both go to zero (Fig. 3). The improvement over the reference method is clear.

Although the method is based on inviscid characteristic theory, it also works very well for viscous flows, like the Poiseuille flow. All tests are presented in Poinsot and Lele (1989).

2. Applications to premixed turbulent flames

2.1. The effect of pressure waves on flame propagation

The effects of pressure waves on combustion and especially the effects of acoustic waves on the stability of a reacting flow are not well understood at the present time although their practical importance is evident in many situations (Yang and Culick 1986, Poinsot et al 1987, 1988). Some of these effects can be simulated numerically. One of the most interesting configurations is the premixed flame in a shear layer (Fig. 4 to 6). This case illustrates also the importance of the boundary conditions which control the acoustics. Depending on the boundaries, the flame will behave very differently:

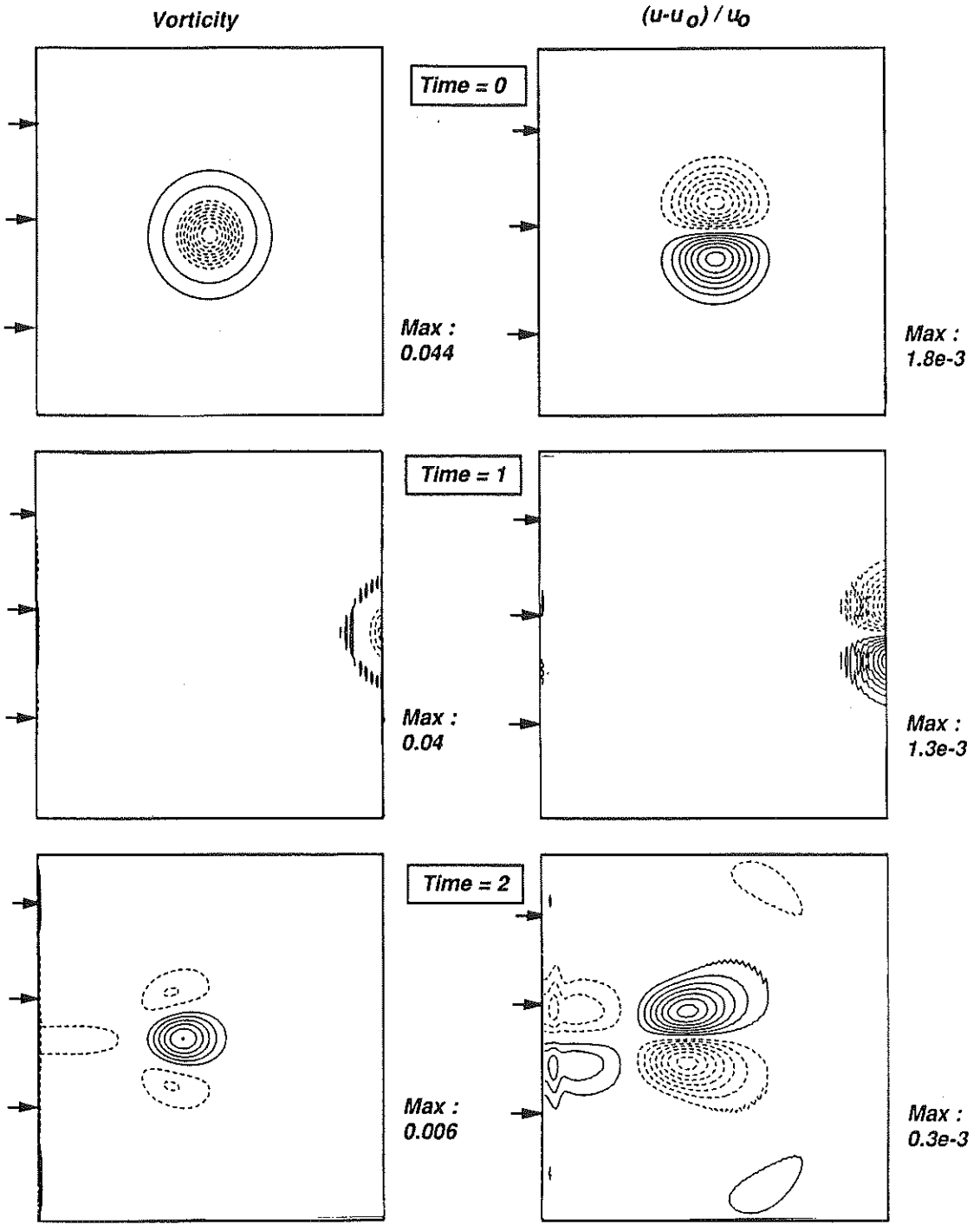

FIGURE 1. Transmission of a vortex through a non-reflecting boundary. Reference method.

- if all boundaries are non-reflecting (Fig. 4), acoustic waves will leave the domain and no coupling may take place between combustion and acoustic waves. The total reaction rate in the computation box will reach a constant value after a finite time and a steady state is obtained.

- if the flame is placed in an infinite duct, where no reflection is allowed at the downstream end but where walls are placed on each side of the shear layer, no steady state is obtained (Fig. 5). The reaction rate oscillates and the frequency of oscillation (obtained by a non-linear spectral method (Veynante and Candel 1988)) is the frequency f_{2t} of the second transverse acoustic mode of the duct. This mode has a pressure antinode near the duct axis, where the flame is spreading, and this condition, known as the Rayleigh criterion, is necessary to have coupling between combustion and acoustic waves.

- finally, if the flame is placed in a 'real' duct with walls and reflection on a downstream end of the tube, the reaction rate oscillations are dominated by the quarter-wave mode of the duct at frequency f_{1L} (Fig. 6). The second transverse mode of the duct (frequency f_{2t}) is also present as indicated by spectral analysis (Fig. 7a). Although the reaction rate and the quarter-wave mode are directly coupled, the vorticity oscillations are insensitive to the quarter-wave mode (Fig. 7b). They depend only on the transverse modes f_{1t} and f_{2t}. The flow structure in this case is displayed in Fig. 8. The fuel concentration field (Fig. 8a) shows that the flame front is wrinkled. (These wrinkles do not appear when no acoustic wave is present, for example for the case of Fig. 4). Structures are convected along the flame front at the flow speed. The vertical velocity contours (Fig. 8b) reveal that they are formed at the duct inlet by the sloshing motion due to the acoustic transverse oscillations.

This simple example shows that a strong coupling may occur between acoustic waves and combustion. This interaction is believed to be even stronger when the flame front reaches a wall. More studies of these mechanisms will be performed in the coming year.

2.2. The interaction between flame fronts and vortices

The modeling of turbulent premixed combustion is still largely based on empiricism because of the complexity of flame/turbulence interactions. The first step in building a turbulent combustion model is to determine in which combustion regime the reacting flow will be. Diagrams defining combustion regimes versus length and velocity scales ratios have been proposed by Borghi (1984), Peters (1986), Bray (1980) and Williams (1985). Knowing the integral turbulence scale and the turbulent kinetic energy, these diagrams indicate if the flow will contain flamelets, pockets or distributed reaction zones. Each of these regimes requires specific modeling.

In the 'flamelet' domain, chemical times are small compared to turbulence times (Bray 1980). Eddies stretch and convolute the flame front, but they do not destroy its internal structure. The flame front can be described as a laminar

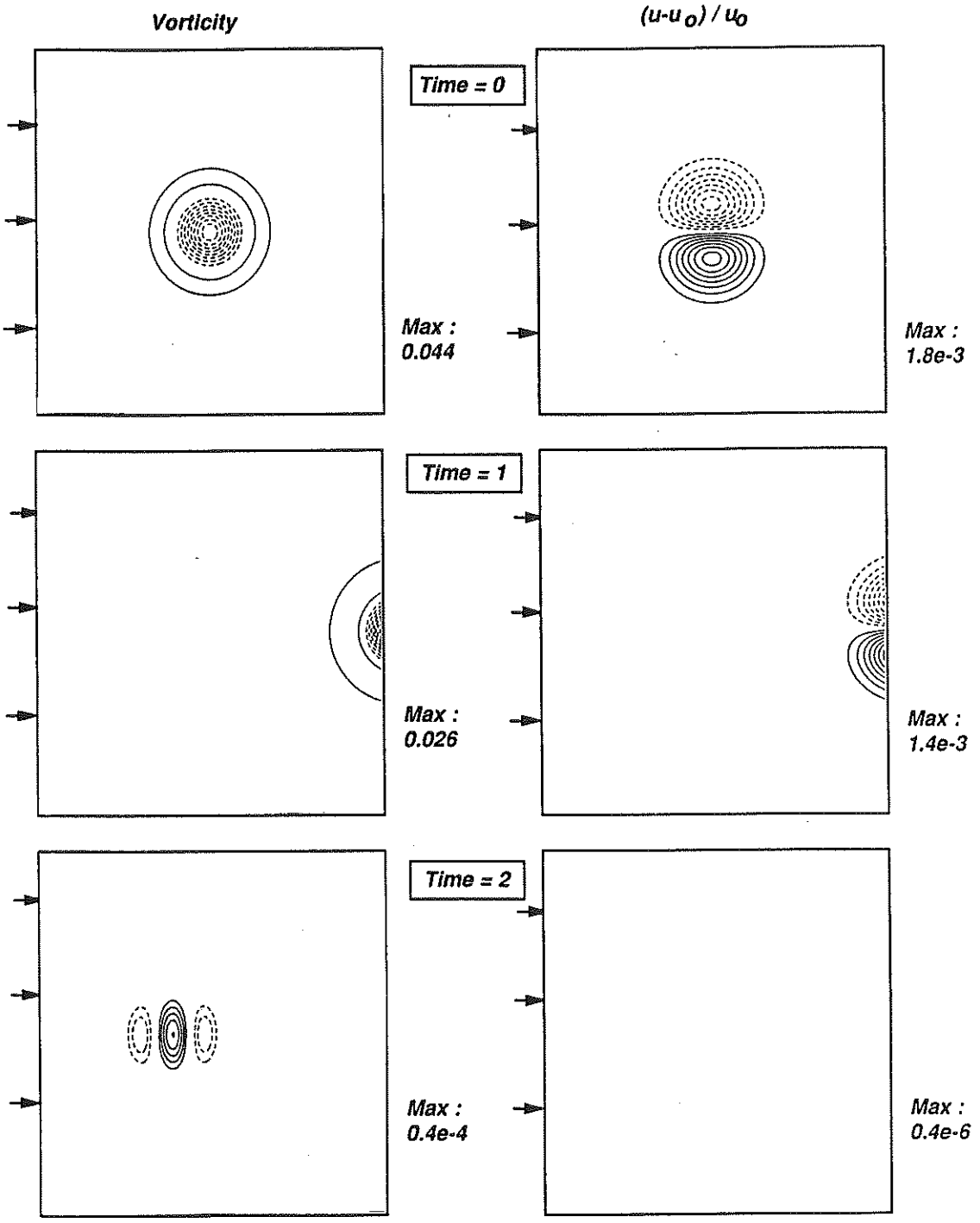

FIGURE 2. Transmission of a vortex through a non-reflecting boundary. NSCBC method.

flame between fresh and burnt gases. The modeling of such a flow is done by tracking the area of this interface (Candel et al 1988, Veynante et al 1989).

In distributed reaction regimes, the turbulence is very intense, and the flame is shred in small elements. No laminar flame front can be identified any more. Statistical models (Pope and Cheng 1987, Borghi 1984) are likely to be better adapted.

Therefore, knowing which regime corresponds to the flow to be modelled is a necessary and important step in turbulent combustion modeling. Unfortunately, the dimensional analysis which is used to construct these diagrams is rather crude and neglects important effects such as flame front curvature, transient or viscous effects. The basic reason for this situation is that these mechanisms are not well understood and, therefore ,are ignored in this first-order analysis.

It is possible to construct realistic turbulent combustion diagrams. The technique which was used here is based on a detailed analysis of the physical mechanisms controlling turbulent premixed combustion and uses direct numerical simulation to quantify them (Poinsot, Veynante and Candel 1990). This is done by constructing a 'spectral' diagram describing the interaction between one isolated vortex and a laminar flame front. This information is used afterwards to infer the behavior of a complete turbulent reacting flow and construct more quantitative diagrams.

2.2.1. Turbulent combustion diagrams

Classical turbulent combustion diagrams suppose that a reacting flow can be parameterized using two non-dimensionalized numbers: the ratio of the turbulence integral scale l to the flame front thickness l_F and the ratio of root-mean-square velocity fluctuations u' to the laminar flame speed s_L. Using the notations and assumptions of Peters (1986), different transitions can be associated to specific lines in this diagram (Fig. 9a).

- The line $u'/s_L = 1$ indicates the transition between wrinkled flames and corrugated flames (flames where turbulence can form pockets of fresh gases in burnt gases).
- The limit between flamelets and distributed reaction zones is reached when the stretch $\frac{1}{A}\frac{dA}{dt}$ (A is the flame surface) imposed on the flame becomes larger than the critical stretch for extinction and creates local quenching. The critical stretch depends on the flame characteristics but may be estimated by s_L/l_F (Peters 1986). Defining the Karlovitz number by:

$$Ka = \frac{\frac{1}{A}\frac{dA}{dt}}{s_L/l_F}, \tag{2}$$

we expect local quenching and distributed reaction zones if $Ka > 1$.

The flame stretch $\frac{1}{A}\frac{dA}{dt}$ can be expressed as a function of the Taylor scale Λ and of u' as

$$\frac{1}{A}\frac{dA}{dt} \simeq u'/\Lambda.$$

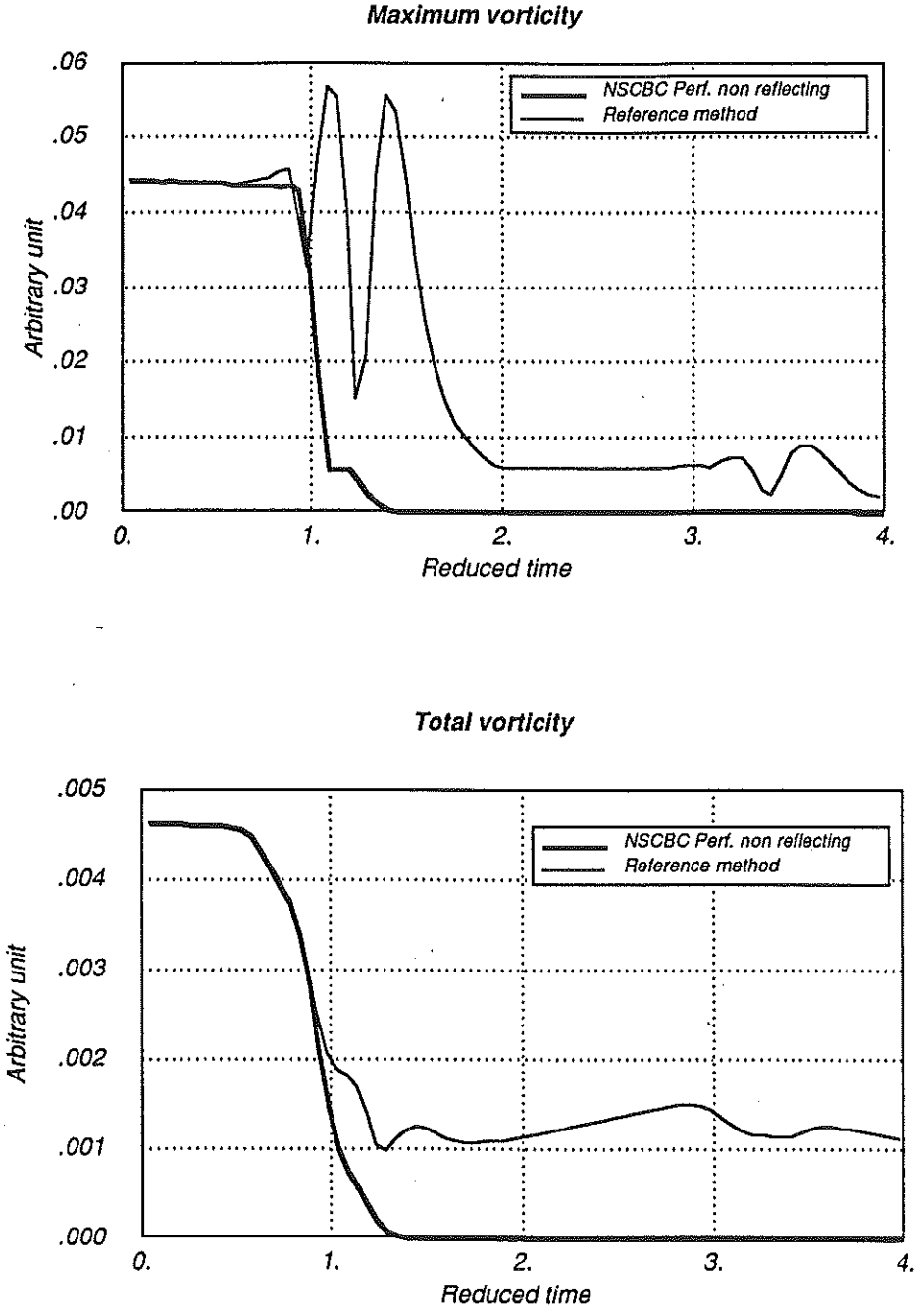

FIGURE 3. Transmission of a vortex through a non-freflecting boundary. Comparison between reference and NSCBC methods.

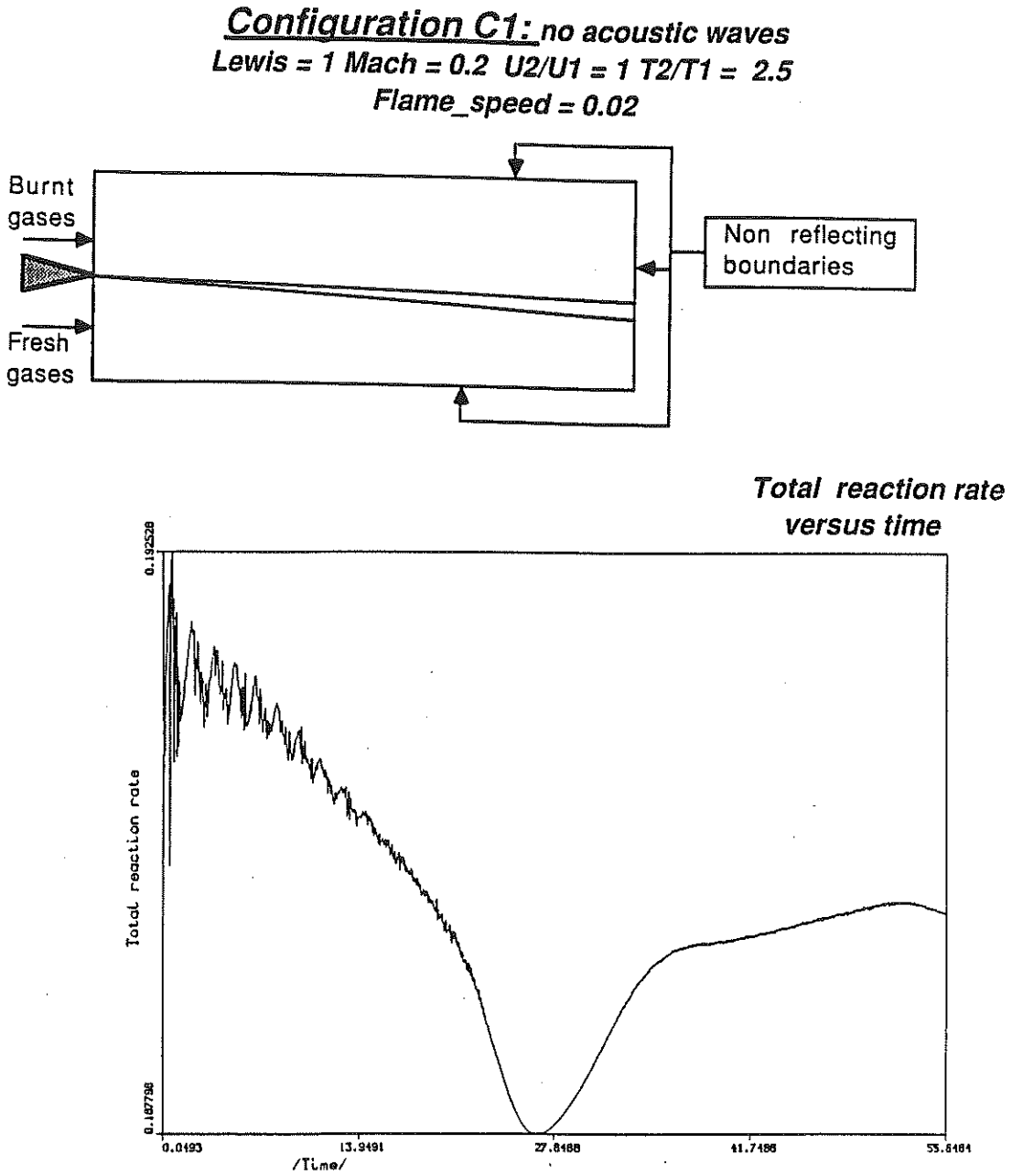

FIGURE 4. Reacting shear layer in an infinite domain.

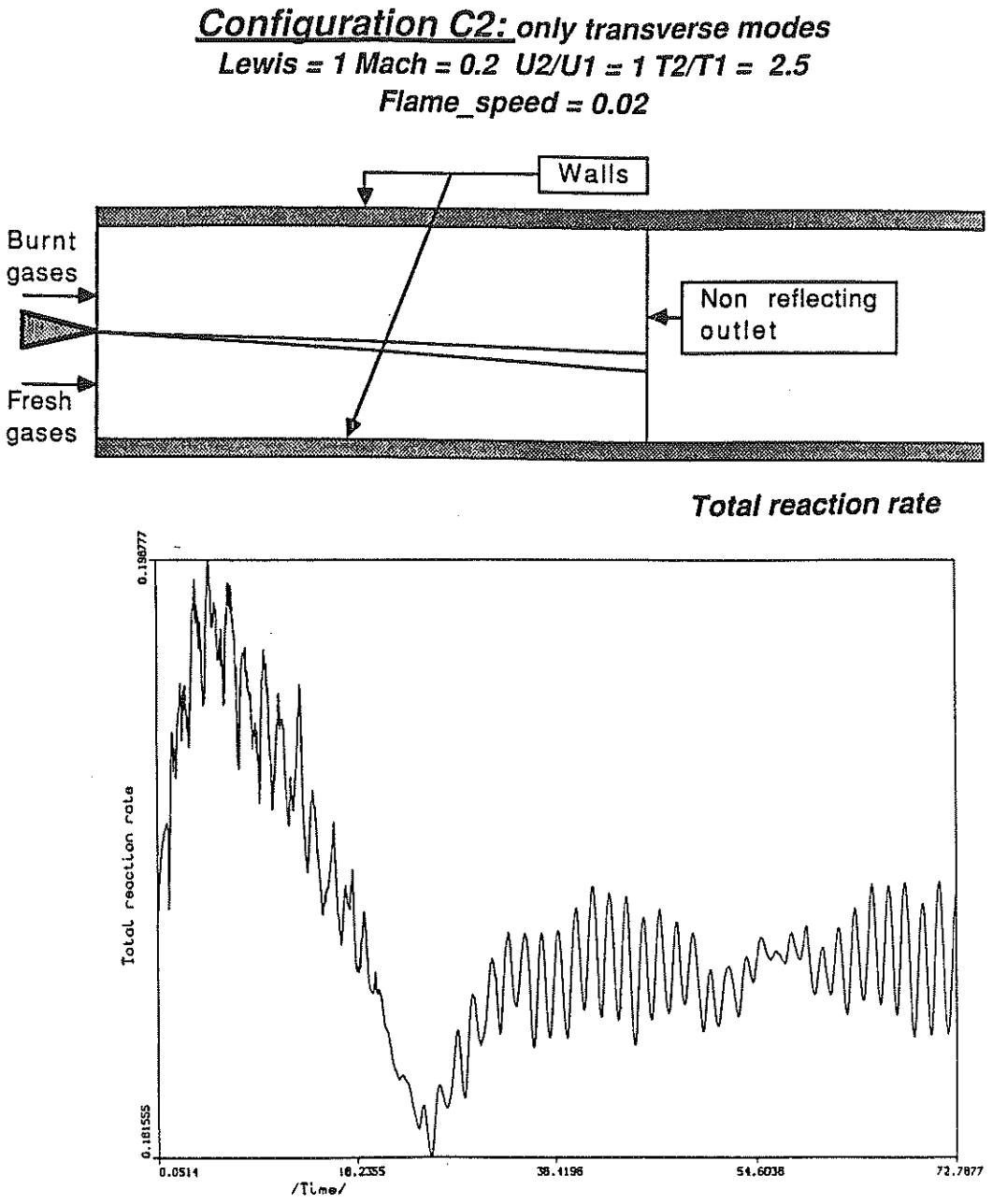

FIGURE 5. Reacting shear layer in an infinite duct.

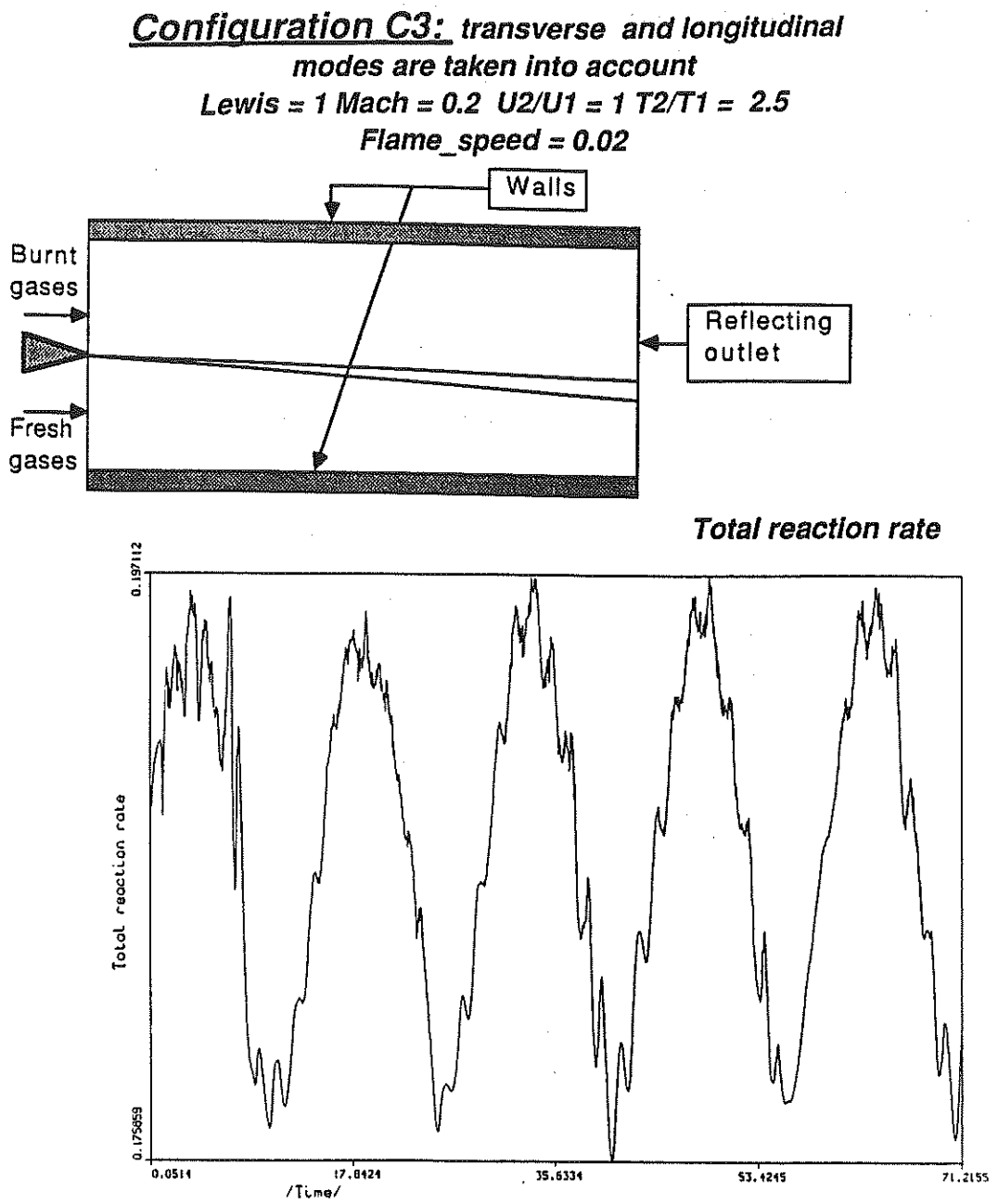

FIGURE 6. Reacting shear layer in a finite duct.

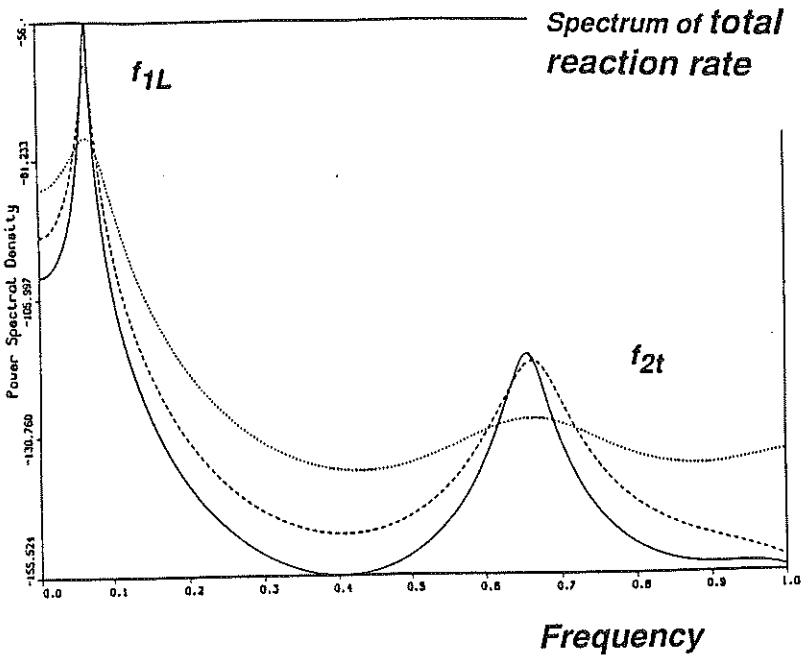

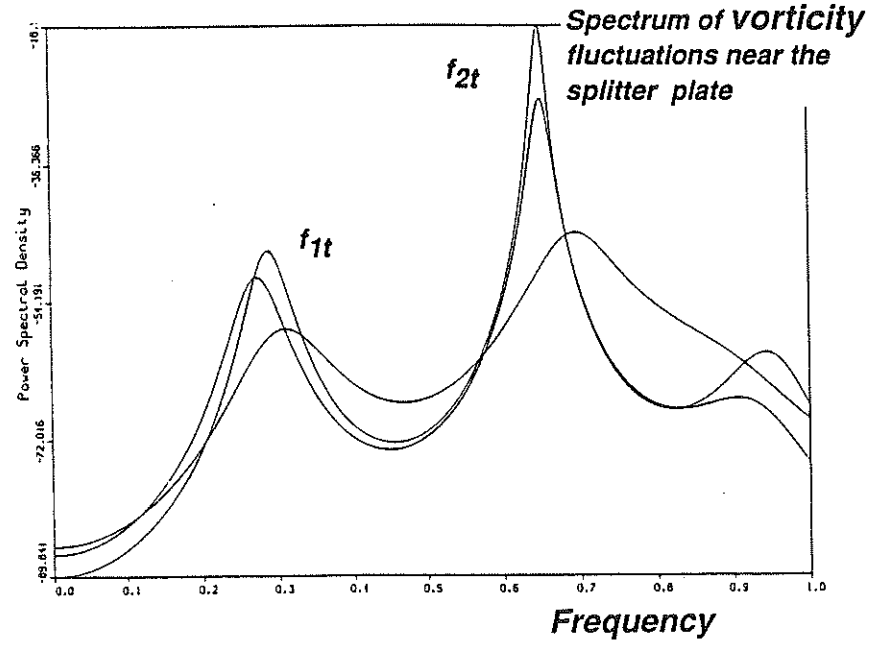

FIGURE 7. Reacting shear layer in a finite duct. Spectral analysis of total reaction rate and vorticity near the splitter plate.

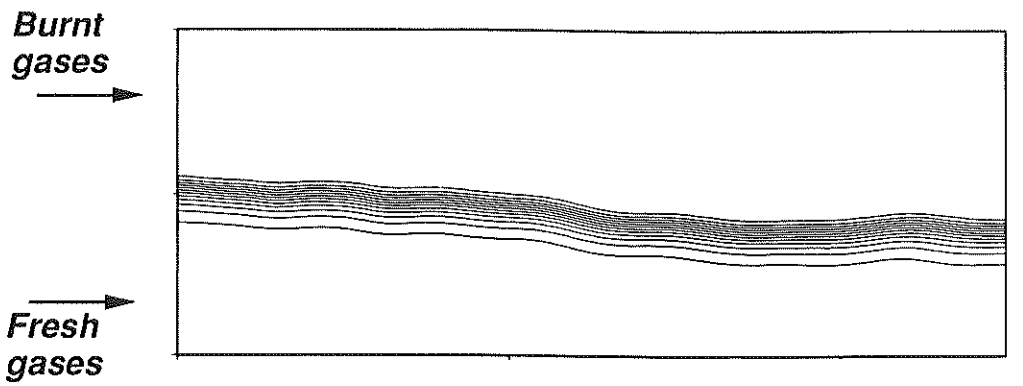

(a) Fuel mass fraction

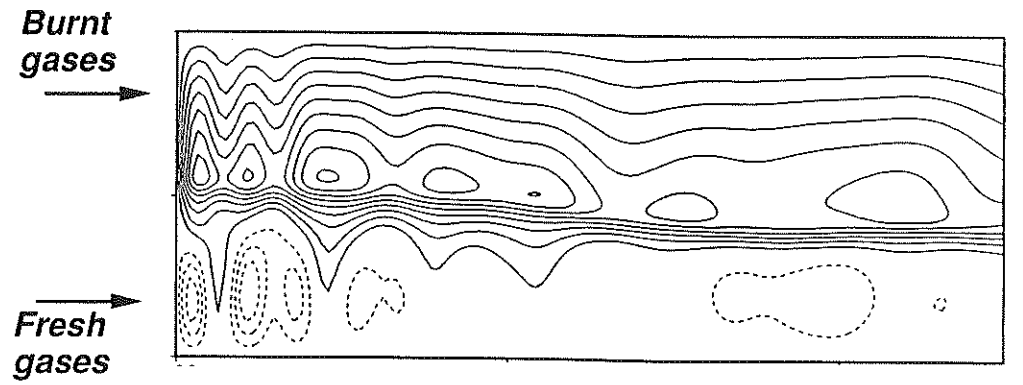

(b) Vertical velocity

FIGURE 8. Reacting shear layer in a finite duct. Flow field at time = 70.

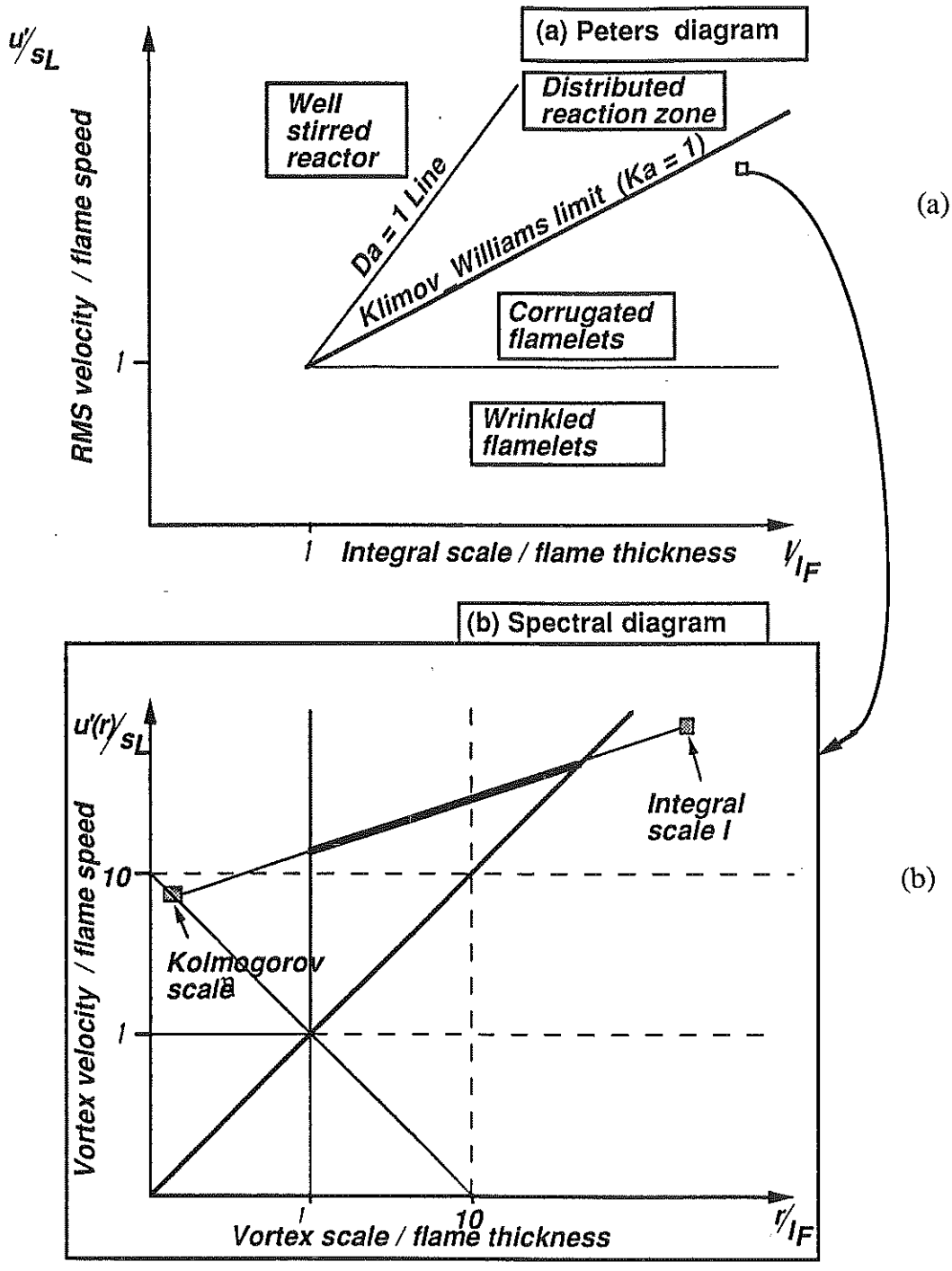

FIGURE 9. Diagrams of premixed turbulent combustion: (a) Standard diagram (with Peters notations); (b) Spectral diagram.

Using the definitions of the Taylor scale Λ and of the Kolmogorov scale η, we can construct four expressions for Ka:

$$Ka \simeq \left(\frac{(u'/s_L)^3}{l/l_F} \right)^{1/2} = \frac{\sqrt{\epsilon/\nu}}{s_L/l_F} = \left(\frac{l_F}{\eta}\right)^2 = \frac{u_K/\eta}{s_L/l_F}. \quad (3)$$

where u_K is the characteristic speed of Kolmogorov scales.

The Klimov-Williams (KW) criterion is then obtained by considering the third expression of the Ka number in Eq. (3) and stating that no flamelet should be observed in a reacting flow if the Kolmogorov scale η is smaller than the flame thickness l_F. According to the KW criterion, no flamelets would exist beyond $Ka = 1$ because their internal structure would be destroyed by stretching and quenching. The $Ka = 1$ limit is a line with a slope 1/3 in the diagram of Fig. 9a (Eq. (3)). The region below $Ka = 1$ is the flamelet region. Note from the last relation in (3) that $\frac{1}{A}\frac{dA}{dt}$ is the strain rate at the Kolmogorov scale: u_K/η. Therefore, the KW criterion is related to only one scale: the Kolmogorov scale.

• Increasing the turbulence intensity beyond the $Da = (u'/l)/(s_L/l_F) = 1$ limit leads to cases where all turbulence times are smaller than the chemical time. This regime, called the well-stirred reactor, is not well understood at the present time.

2.2.2. A spectral diagram for turbulent combustion regimes

The approach used to build diagrams in the previous section has many deficiencies: it considers only one length scale to describe turbulent combustion, it neglects all viscous and transient mechanisms as well as curvature effects. These deficiencies are especially clear when the KW criterion is derived: in Eq. (3), the KW criterion considers the Kolmogorov scales as the most active because they generate the highest strains. This approach ignores three important points:

1- Kolmogorov scales might be too small compared to the flame front thickness to stretch it.

2- Viscous effects might dissipate Kolmogorov scales before they quench the flame front.

3- Scales smaller than the flame front may induce high local curvature and thermodiffusive effects which might counteract the effects of strain.

Using direct simulation, we can derive criterions including viscous and curvature effects and take all length scales into account. The first step is to recognize that turbulent combustion diagrams are obtained through drastic simplifications and begin our analysis from a more basic point of view.

Let us consider first one flame front interacting with one 'turbulent' flow. Supposing that turbulence and chemistry are fixed, we can define a *spectral diagram* which maps the interaction between one of the turbulence scales and the flame front (Fig. 9b). There is one spectral diagram for each point of the Peters diagram.

In this spectral diagram, three classes of vortices can be isolated because they indicate important transitions: the vortices which can form pockets on the wrinkled flame front; the vortices which can quench locally the flame front; the vortices which are too small to interact with the flame zone.

It is important to emphasize that, in the same turbulent reacting flow, all three types of vortices may be found at the same time. The flow structure is the superposition of all vortices and describing it by using only one scale can not take all mechanisms into account. These three effects (pockets formation, quenching, and vortex decay) can be characterized by three non-dimensionalized numbers which depend on the length scale r (r will vary between the Kolmogorov scale η and the integral scale l):

1- $Vr(r) = u'(r)/s_L$ is the ratio of the turbulent velocity fluctuations associated with the length scale r to the laminar flame speed.

2- $Ka(r) = \frac{u'(r)/r}{l_F/s_L}$ is the Karlovitz number for the scale r. It reduces to the Karlovitz number Ka of Eq. (3) if $r = \eta$.

3- $Po(r) = \frac{r^2 s_L}{\nu l_F} = (\frac{r}{l_F})^2$ is a measure of the power of the vortex. It is the ratio of the life-time of the vortex r^2/ν to the chemical time l_F/s_L. It can also be interpreted as the ratio of the penetration length of the vortex into the flame front (before it gets dissipated by viscous effects) to the flame front thickness. It is also a good measure of the curvature effects.

In the spectral diagram, a turbulent flow field is represented by a straight line (called here 'turbulence line') bounded by the Kolmogorov and the integral scales.[a] Kolmogorov scales are located on the line $Re_\eta = u'(\eta)\eta/\nu = \frac{u'(\eta)}{s_L}\frac{\eta}{l_F} = 1$.

Each point of the turbulence line corresponds to the interaction of one length scale with the flame front (Fig. 9). Such an interaction may be computed exactly and an accurate spectral diagram may be constructed as we will show in the next section.

2.2.3. Direct simulation of vortex/flame front interactions

Many authors have studied vortex/flame interactions (Cetegen and Sirignano 1988, Ghoniem and Givi 1987, Laverdant and Candel 1988, Ashurst et al 1987). However, very few have considered all mechanisms which should be taken into account to determine turbulent combustion regimes. This is done here by solving the Navier-Stokes equations in a two-dimensional configuration using the assumptions described in Section 2.1.

The configuration is the following (Fig. 10a): at $t = 0$, two counter-rotating vortices are generated upstream of a laminar flame front. The flow is symmetrical along the $y = 0$ axis and subsequently, only the upper half is calculated and

[a] We will assume here that the turbulent reference quantities correspond to the fresh gases and that the turbulent spectrum in this part of the flow can be described by the Kolmogorov relation: $u'(r)^3/r = \epsilon$ where ϵ is the dissipation rate.

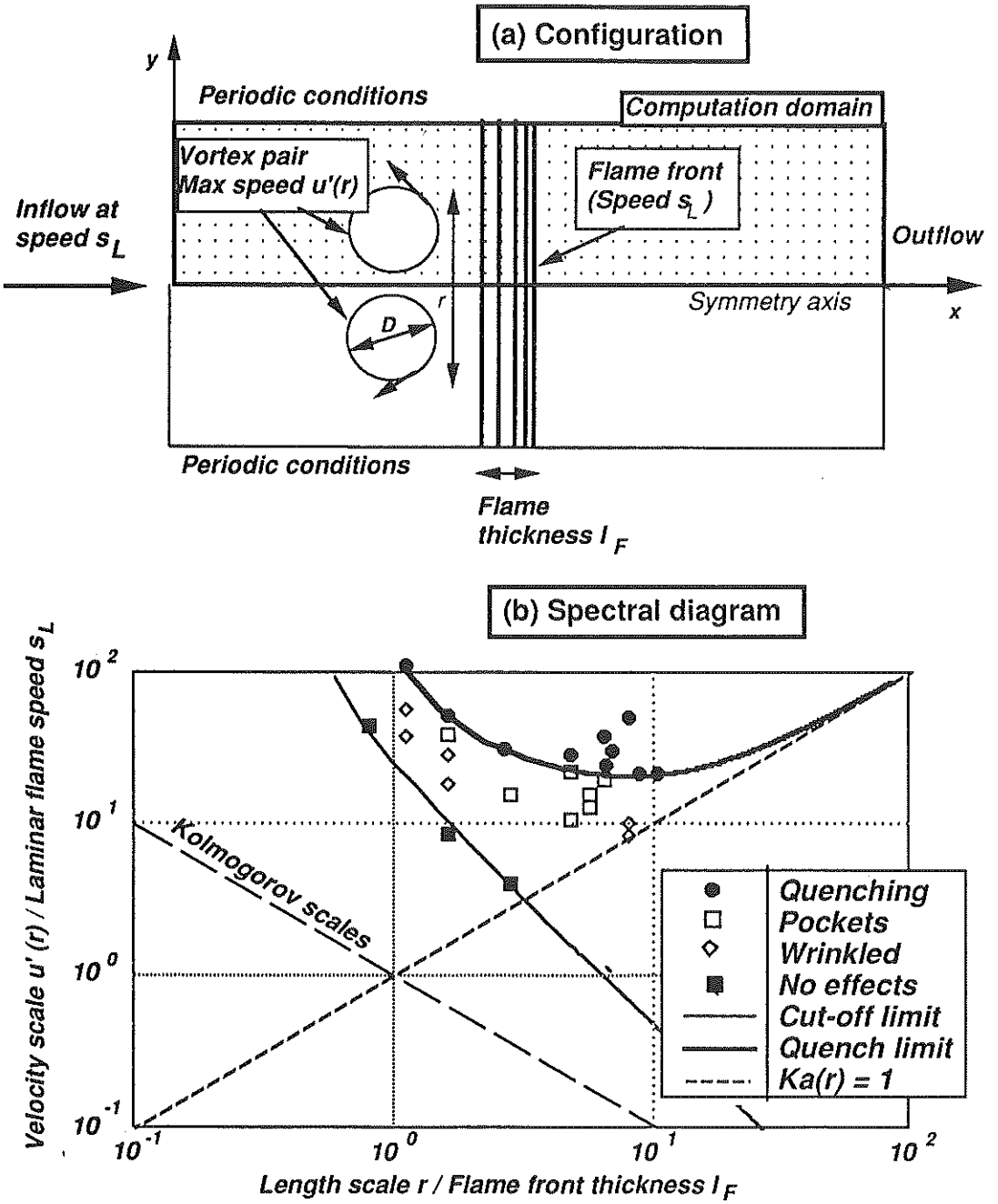

FIGURE 10. (a) Configuration for direct simulation of the interaction between a flame front and a vortex pair; (b) Spectral diagram based on direct simulation results.

displayed. The inlet flow speed is equal to the laminar flame speed so that the flame does not move when it is not perturbed. The vortex-pair configuration allows an accurate measurement of the flame stretch and speed on the axis. It also generates a high stretch and may be considered as one of the most efficient structures able to interact with the flame front because of its self-induced velocity. Finally, it is easy to generate in an experiment and some results on the interaction of a vortex pair with a flame front are available (Jarosinski et al 1988).

Simulations were performed for a flame with a temperature ratio of 4, a flame speed $s_L/c = 0.012$ and a Lewis number of 1.2 (Poinsot et al 1990). The flame front thickness l_F is $3.7\nu/s_L$. The length scale r used to characterize the vortex pair is the sum of the vortex diameter D and of the distance between vortex centers (Fig. 10a). The velocity scale $u'(r)$ is the maximum velocity induced by the pair. Tests have been performed for $0.81 < r/l_F < 11$ and $1 < u'(r)/s_L < 100$.

2.2.4. The spectral diagram and the new turbulent combustion

The resulting spectral diagram is displayed in Fig. 10b. Depending on the scale r and on the vortex pair maximum velocity $u'(r)$, computation shows that the interaction can lead to different results:

- a local quenching of the front (with or without pocket formation),
- the formation of a pocket of fresh gases in the burnt gases without quenching,
- a wrinkled flame front
- a negligible global effect without noticeable flame wrinkling or thickening.

Two lines have been constructed in this diagram: the quenching limit and the cut-off limit.

• The quenching limit indicates vortices able to quench the flame front. It was fitted among our data points for $0.81 < r/l_F < 11$ and extended for large scales $r/l_F > 11$ to match the line $Ka(r) = 1$ (Large vortices stretch the flame front like in a stagnation point flow: stretch is sustained for long times and little curvature is induced. Therefore, quenching by these structures is only determined by the ratio of vortex-induced stretch to critical flame stretch and occurs when $Ka(r) = 1$.)

• The cut-off limit corresponds to vortices inducing a modification of the total reaction rate of less than 5 percent.

From the spectral diagram, it is possible to construct a premixed turbulent combustion diagram by using the following assumptions:

(1) there are no interactions between vortices of different size,

(2) only one vortex interacts at a given time with the flame front,

(3) any structure located in the quenching zone of the spectral diagram will quench locally the flame front and induce a distributed reaction regime.

These assumptions are rather simple. The energy spectrum, for example, certainly plays an important role: scales in the quenching zone will not quench

the flame front if the energy density for these scales is too low. Therefore, assumption (3) is probably not satisfied. However, these hypothesis lead to a 'maximal' interaction diagram. Experimental results would probably lead to higher limits of $u'(r)$ for the first distributed reaction zones.

An important limitation of the present approach appears for very small and energetic scales. In this region, the effect of many small vortices on the flame front is difficult to deduce from the effect of one isolated vortex. Studying well-stirred combustion would require to take a complete turbulent field into account.

Under the assumptions listed above, the construction of a turbulent combustion diagram is straightforward. A turbulent field of type B (Fig. 11a) will contain inefficient scales (dashed line) and scales able to have some effect on the flame front but unable to quench it (solid line). Point B will, therefore, correspond to a flamelet regime. In the case of field A, even the integral scale will not be energetic enough to interact with the flame front, and the latter will remain pseudo-laminar. Turbulent field C contains scales able to quench locally the flame front (double-width solid line). Note that these scales are larger and faster than the Kolmogorov scale by orders of magnitude. C will correspond to a distributed reaction zone. The limit of distributed reaction zones is obtained by taking the tangent with a slope of 1/3 to the quenching limit of the spectral diagram. Comparing this diagram (Fig. 11b) with the Peters diagram (Fig. 9a) reveals that the domain where distributed reaction zones may be expected has moved at least of an order of magnitude towards more intense fields. The heat losses used for this computation were quite high (see Fig. 13) and in most practical cases, with lower heat losses, we expect the flamelet domain to be even larger than the present one.

Different characteristic scales may be extracted from the spectral diagram. For example, the cut-off and the quenching scales introduced by Peters (1986) can be evaluated from the quantitative data of Fig. 13 and are different by orders of magnitude when compared with the estimates given by Peters. Quenching criteria can also be derived (see Poinsot et al 1990).

2.2.5. An example of flame quenching by a vortex pair

To illustrate direct simulation results, we will describe a case where the vortex pair size and speed are high enough to induce quenching of the flame front ($r/l_F = 18$ and $u'(r)/s_L = 28$). Figures 12 and 13 display the reaction rate ($\dot{w}$) and the temperature (Θ) fields at four instants. Time is normalized by the flame time l_F/s_L: $t^+ = ts_L/l_F$.

The interaction is fast and ends after about two flame times. At $t^+ = 0.65$, the vortex pair has stretched and curved the flame but its inner structure is preserved and no quenching is observed. The Karlovitz number at this instant on the symmetry axis is around three. The fact that the flame is still burning despite such a high Karlovitz illustrates the importance of transients. At $t^+ = 1.3$, quenching appears on the downstream side of the pocket of fresh gases formed

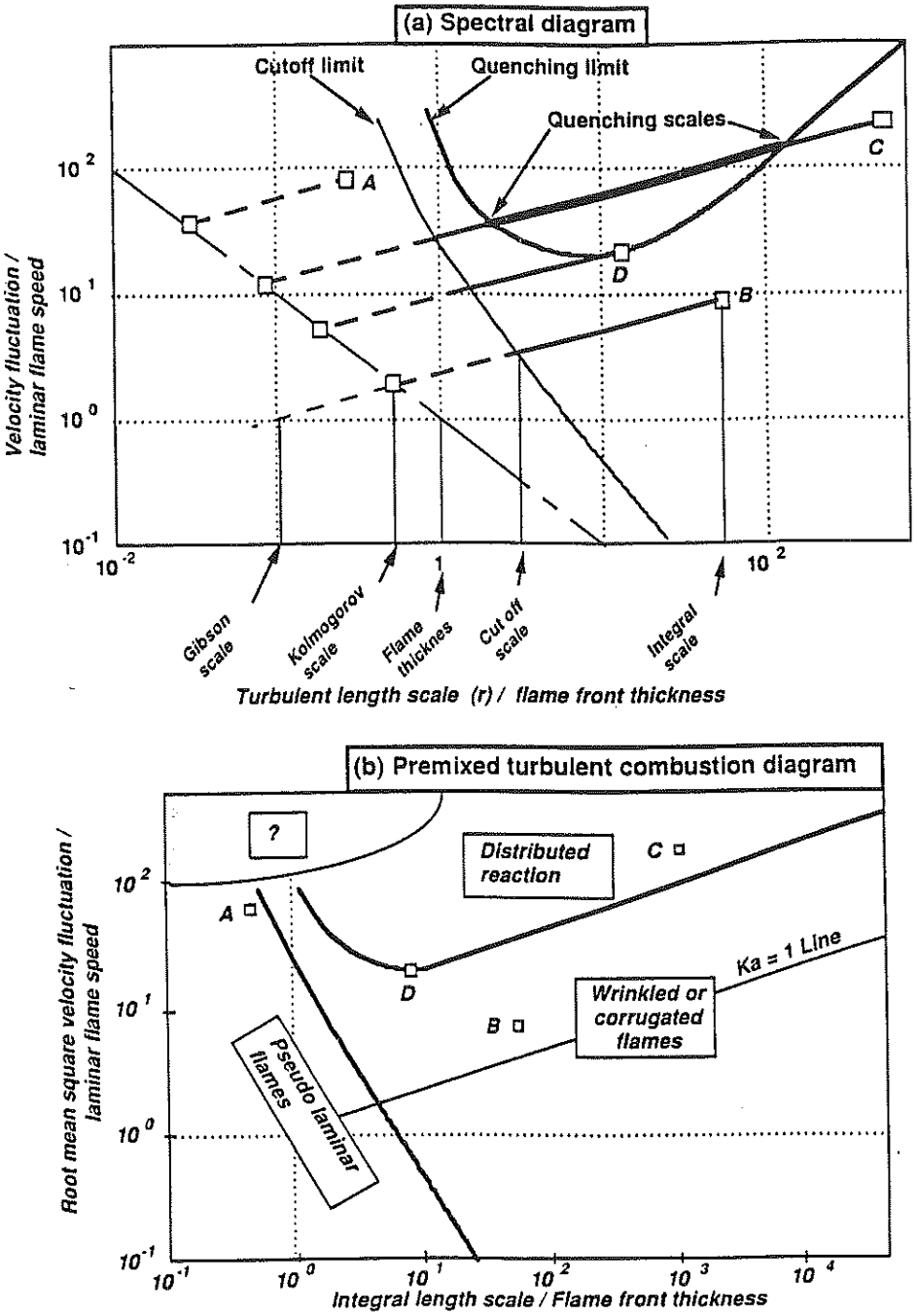

FIGURE 11. Construction of the diagram for pemixed turbulent combustion using the spectral diagram. Lewis = 1.2, strong heat losses.

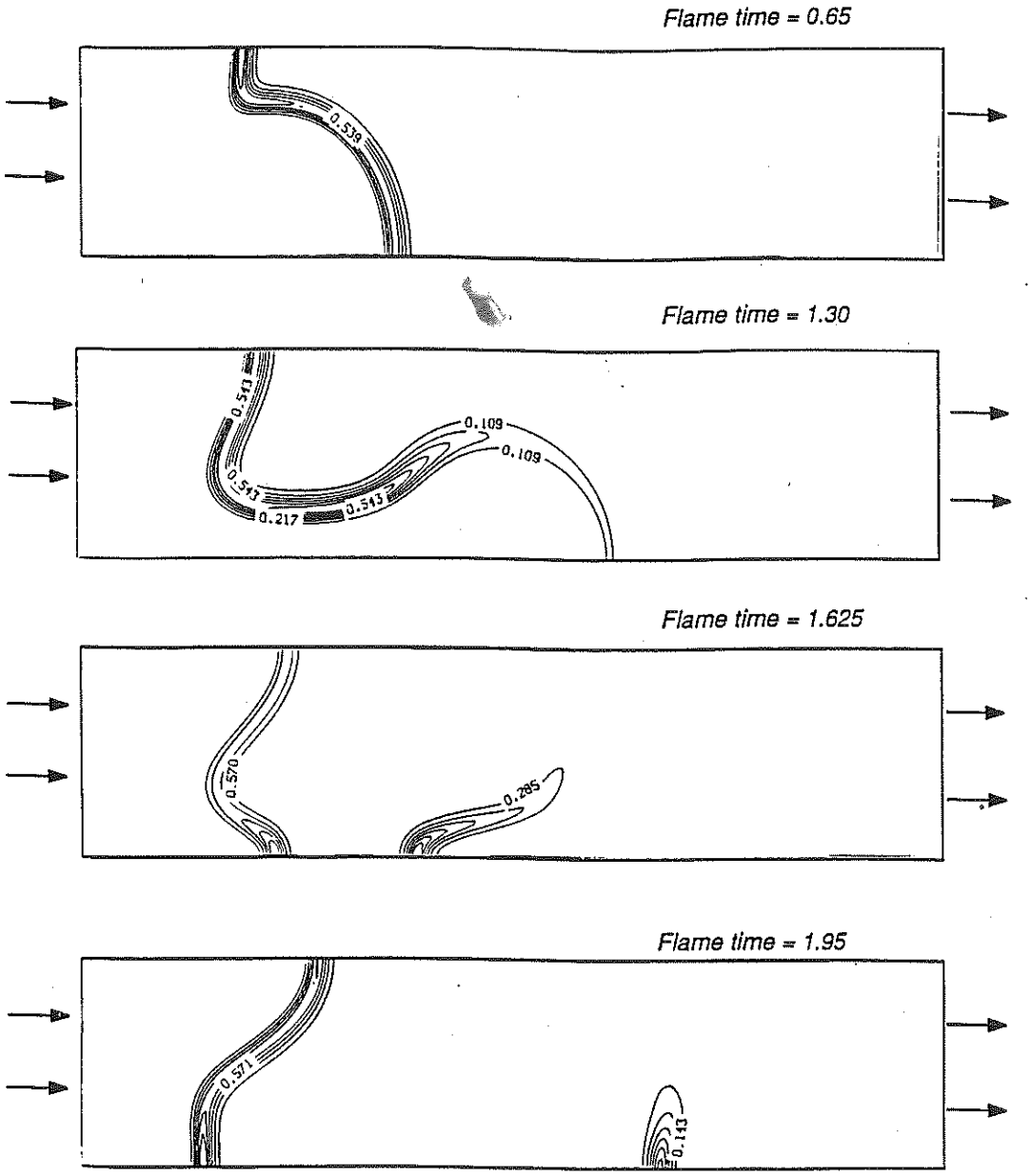

FIGURE 12. Instantaneous reaction rate fields at four instants. Quenching occurs at the tip of the flame at time = 1.30. $r/l_F = 18$ and $u'(r)/s_L = 28$.

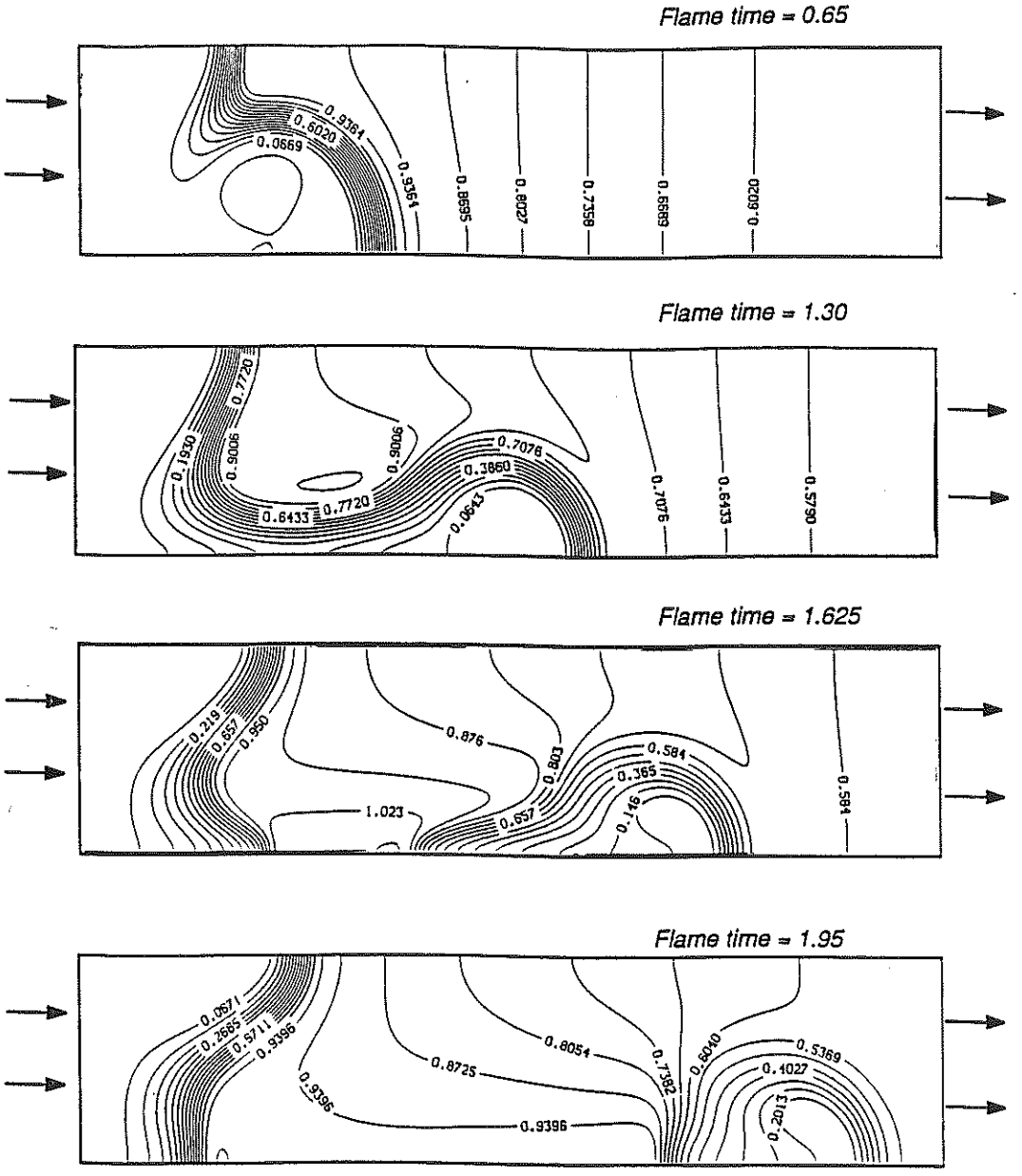

FIGURE 13. Instantaneous temperature fields at four instants. A pocket of fresh gases is formed i the stream of the burnt products. $r/l_F = 18$ and $u'(r)/s_L = 28$.

by the vortex pair. These gases are pushed rapidly into regions where the burnt gases have been cooled due to heat losses (Fig. 13). This effect, combined with the high stretch generated by the vortices, causes almost complete extinction of the pocket after it has been separated from the bulk of the fresh gases. At times $t^+ = 1.625$ and 1.95, the pocket of fresh gases is convected through the burnt gases without burning except near its tail. In this case, the flame front is not only quenched locally by the vortex pair, in addition, unburnt mixture is able to cross the flame. This mechanism may be associated with pollutant formation (i.e unburned hydrocarbons in automobile exhausts).

To conclude, the direct simulation code used in this work appears to be a powerful tool to study turbulent combustion. Possible problems to be studied in the future year include the following :

- the extension of spectral diagrams to Lewis numbers lower than unity,
- the response of the flame front to an ensemble of small energetic vortices,
- the effect of the flame front on the vorticity field.

3. The influence of curvature on premixed flame fronts

The previous section shows that curvature is an important parameter in turbulent combustion. A convenient geometry to isolate the effects of curvature in a steady reacting flow is the tip of a Bunsen burner. This zone is highly curved and depending on the chemistry and on the flow speed, the flow speed upstream of the flame front can be five to fifteen times the laminar flame speed. Many experimental studies have been performed on flame tips (see for example Mizomoto et al 1984). In a collaborative work with Dr. Mungal and T. Echeckki, who have done a flame tip experiment at Stanford, I have started computations of flame tips for different Lewis numbers and have found interesting results. In particular, for Lewis numbers lower than unity, the flame tip opening phenomenon, where the flame is quenched at the flame tip, is correctly captured by the code. This study will be pursued by writing a one-dimensional code able to predict the combined effects of stretch and curvature on a flame and comparing its results with the two-dimensional computation and with measurements.

4. The validation of flamelet models for premixed turbulent combustion

The validation of flamelet models is an important aspect of the present work. Two approaches are used.

First, the fundamental information obtained on flame / vortex interactions are incorporated in the model. The existence of quenching, the dynamics of the pockets, the effects of transients, and viscous dissipation constitute a valuable source of guidelines to construct a model. For example, the fact that scales smaller than the flame front thickness have almost no effect on the flame front (as evidenced from the spectral diagram of Fig. 11a) allows a much simpler modeling of the flame front. It also indicates which strain should be used to quantify

the flame area increase due to turbulence. Clearly the value of $\sqrt{(\epsilon/\nu)}$ which corresponds to the strain at the Kolmogorov scale overestimates the effective flame stretch. A second obvious result is that the spectral diagram obtained in Fig. 11a would be completely different if the Lewis number was lower than unity. In this case, stretch would increase the flame speed while curvature would promote extinctions. The Lewis number must be a central parameter in any turbulent combustion model. This conclusion is similar to the one obtained by Abdel-Gayed and Bradley (1985) from experimental results.

Second, once a model is built, direct simulation can be used to test it and adjust 'constants'. This was done in collaboration with Dr. D. Veynante in September 1989. The Coherent Flame Model (Candel et al 1988) and the stochastic model of Pope and Cheng (1988) were compared to direct simulation results. Realizability of both models was also considered. This study will be continued in 1990.

REFERENCES

ABDEL-GAYED R. G. & BRADLEY D. 1985 *Comb. and Flame* **62**, 61-68

ASHURST W. T., PETERS N. & SMOOKE M. D. 1987 *Combust. Sci. and Tech* **53**, 339-375

BORGHI R. 1984 *Recent Advances in Aeronautical Science*, C. Bruno, C. Caseci (Eds), Pergamon

BRAY K. N. C. 1980 *Topics in Applied Physics*, P. A. Libby and F. A. Williams ed. Springer Verlag

BUELL J. & HUERRE P. 1988 *Proceedings of the Summer Program 1988, Center for Turbulence Research* 19-27

CANDEL S., MAISTRET E., DARABIHA N., POINSOT T., VEYNANTE D. & LACAS F. 1988 Marble Symposium, CALTECH, Pasadena

CETEGEN B. & SIRIGNANO W. 1988 26th AIAA Aerospace Sciences Meeting, AIAA Paper 88-0730

GHONIEM A. AND GIVI P. 1987 25th AIAA Aerospace Sciences Meeting, AIAA Paper 87-0225

JAMESON A. & BAKER T.J 1984 AIAA 22nd Aerospace Sciences Meeting, AIAA Paper 84-0093

JAROSINSKI J., LEE J., KNYSTAUTAS R. 1988 *Twenty Second Symposium (International) on Combustion.* The Combustion Institute

MIZOMOTO M., ASAKA Y., IKAI S. & LAW C. K. 1984 *Twentieth Symposium (International) on Combustion.* p. 1933, The Combustion Institute

PETERS N. 1986 *Twenty First Symposium (International) on Combustion.* p. 1231, The Combustion Institute

POINSOT T., TROUVE A., VEYNANTE D., CANDEL S. & ESPOSITO E. 1987 *J. of Fluid Mech.* **177**, 265-292

POINSOT T. & CANDEL S. 1988 *Combus. Sci. Tech.* **61**, 121-153

POINSOT T., VEYNANTE D. & CANDEL S. 1990 submitted to the *Twenty First Symposium (International) on Combustion* The Combustion Institute

POINSOT T. & LELE S. 1989 submitted to the *J. of Comput. Phys.*

POINSOT T., COLONIUS T. & LELE S. 1989 presented at the *42nd A.P.S. Meeting* Division of Fluid Mech.

POPE S. B. & CHENG W. K. 1988*Twenty Second Symposium (International) on Combustion.* The Combustion Institute

RUTLAND C. J. & FERZIGER J. 1989 27th AIAA Aerospace Sciences Meeting. AIAA Paper 89-0127

VEYNANTE D. & CANDEL S. 1988 *Signal Processing* **14**, 295-300

VEYNANTE D., LACAS F., MAISTRET E. & CANDEL S. 1989 7th Symp. on Turbulent Shear Flows. Stanford

WILLIAMS F. A. 1985 *Combustion theory*, 2nd ed. Benjamin Cummings, Menlo Park

YANG V. & CULICK F. E. C. 1986 *Combus. Sci. Tech.* **45**, 1-25

YEE H. C. 1981 *NASA Tech Memo* 81265